Prognosis of the cardiovascular disorder among the type 2 diabetic subjects based on infrared thermal imaging

[*]S Sivanandam

[*]Professor, Department of Biomedical Engineering, Saveetha Engineering College, Chennai, India.

Corresponding Author:

Dr.S.Sivanandam
Professor
Department of Biomedical Engineering
Saveetha Engineering College, Chennai
Tamilnadu, India.
ORCID: 0000-0003-4816-2431

Abstract

Purpose Inflammation plays an essential role in the pathogenesis of atherosclerosis. The study aims to adjunct the standard biomarker, high-sensitivity C-reactive protein test against the non-contact medical thermography for the prognosis of cardiovascular events among diabetic subjects.

Mthods The decrease in the skin surface temperature at the posterior region of the tibia indicated statistical significance. Pearson's positive correlation between the variables HbA_{1c} and hs-CRP was observed among the diabetic subjects.

Results The artificial neural network classifier resulted in an accuracy of 89.8%, a sensitivity of 88%, and a specificity of 91.7%. Among the diabetic subjects, hs-CRP was negatively

correlated with the statistical feature, the entropy that could predict the poor perfusion of the vasculature (R^2=0.622).

Conclusionn The skin surface temperature of the tibial region measured at the anterior (AUC: 0.694) and posterior region (AUC: 0.832) were significant against the hs-CRP, an invasive method. Thus, the thermal imaging method measured at the tibial (posterior) region may aid as a non-invasive screening tool for early diagnosis of cardiovascular events among diabetic subjects.

Keywords: *Type 2 diabetes, Cardiovascular disease, Inflammation, Thermal infrared imaging, high-sensitivity C-reactive protein*

INTRODUCTION

Type 2 diabetes mellitus (DM) has been alarmingly growing worldwide due to its irreversible complications and high prevalence [1]. Clinical evidence indicates that people with type 2 diabetes are at higher risk of macro and microvascular complications. The metabolic abnormalities caused by this disorder lead to vascular dysfunction that inclines the diabetic population to atherosclerosis [2]. According to the American Heart Association (AHA), diabetes is one of the major risk factors for cardiovascular diseases (CVD). Diabetes boosts the incidence of and escalates the prevalence of atherosclerosis [3]. The origin of atherosclerosis is an inflammatory process that leads to vascular endothelium injury [4, 5]. If there is an uncontrolled blood glucose an increased insulin level, the lining cells of the blood vessels not only decrease the production of Nitrous Oxide (NO) but also increase the production of substances that constrict the blood vessel, further encouraging plaque formation [6]. Early detection of atherosclerosis among diabetic subjects is the primary objective in reducing the risk of diabetic vascular complications to aid in decreasing the risk of morbidity and mortality.

The diagnosis of CVD is being carried out based on blood tests, echocardiography, cardiac catheterization, Electrocardiogram (ECG), and cardiac Magnetic resonance imaging (MRI). The gold standard method to diagnose CVD is a lipid profile-based biochemical marker. A lipid profile is a group of blood tests used to assess the risk of developing cardiovascular disease. It consists of high-density lipoprotein (HDL), low-density lipoprotein (LDL), total cholesterol (TC), and triglycerides. Elevated LDL cholesterol and decreased HDL pose a high risk of developing a block in the blood vessels [7]. According to American Heart Association (AHA), a low level of HDL (< 40 mg/dl in Men and <50mg/dl in Women) is highly associated with an elevated risk of CVD. The increased TC/HDL ratio is a better and simpler cumulative marker of the presence of atherogenic dyslipidemia [8].

Low-grade inflammation is a precursor during the pathogenesis of atherosclerosis. The inflammatory biomarker predicts CVD risk at an early stage and is a valuable tool for risk evaluation of cardiovascular events. Based on various epidemiological studies, the most assuring marker for systemic inflammation is high-sensitivity C-reactive protein (hs-CRP) associated with future cardiovascular risk assessment [9]. According to AHA, the reference range of the group is defined as Low risk (hs-CRP <1mg/dl), Intermediate risk (1-3 mg/dl), and High risk (> 3mg/dl) [10]. Thermal infrared imaging is a non-invasive, non-contact, and low-cost imaging modality for determination of the skin surface temperature that measures the thermal infrared energy radiated from the body surface.

Based on the principle of Stefan-Boltzmann law [11].

$$W = \varepsilon \sigma T^4$$

W is the total radiant energy emitted by the human skin surface, ε is the emissivity, σ is the Stefan-Boltzmann constant, and T is the absolute temperature.

The emissivity measures the material's ability to radiate the absorbed energy. Human skin acts as a black body with an emissivity of 0.98 [12]. The body temperature is a good indicator of health; the skin surface temperature difference of 0.5ºC and above in the contra-lateral region indicated possible illness [13]. Medical thermography is a screening tool for various diseases such as breast cancer, diabetes, peripheral vascular disease, and rheumatoid arthritis [14-16]. The limitations of the conventional technique are less accurate, invasive, repeated blood sample extraction is not recommended, the onset of the disorder may go unnoticed until a serious health issue arises. Further, there is no standard biomarker for CVD diagnosis [17, 18].

This study aims to evaluate the potential of medical thermography as a screening tool for the early diagnosis of atherosclerosis among type 2 diabetic subjects through non-invasive means. The present study determined to test the potential of skin surface temperature at the tibial (posterior) region; further, the same ROI was used to extract the features to increase the diagnostic accuracy of this study. The statistical parameters derived from the Statistical Package for Social Science (SPSS) tool and the Gray Level Co-occurrence Matrix (GLCM) features extracted using MATLAB tool from the region of interest (ROI). Figure 1 shows the work flowchart and the study population was classified based on the biomarker, the skin surface temperature measured directly from the Forward Looking Infrared (FLIR) thermal software. Further, the tibial posterior region was selected with ROI through MATLAB tool to extract the GLCM features from the ROI. The neural network model supported by MATLAB tool was used to study the diagnostic efficacy.

A. Subject and Study design

The health screening camp was conducted at SRM Medical College Hospital and Research Centre, Kattankulathur, Tamilnadu, India. The institutional ethical clearance

granted permission to perform the study. Both in-patients and out-patients who participated in this screening camp submitted informed consent forms. A total of N=54 subjects of both genders aged between 24 and 76 years participated in this study. n=5 subjects were excluded from the study due to confounding factors. A detailed questionnaire analyzes the health conditions of the subjects involved in the camp. Subjects with fever, thyroid, and arthritis were excluded based on information procured from the questionnaire.

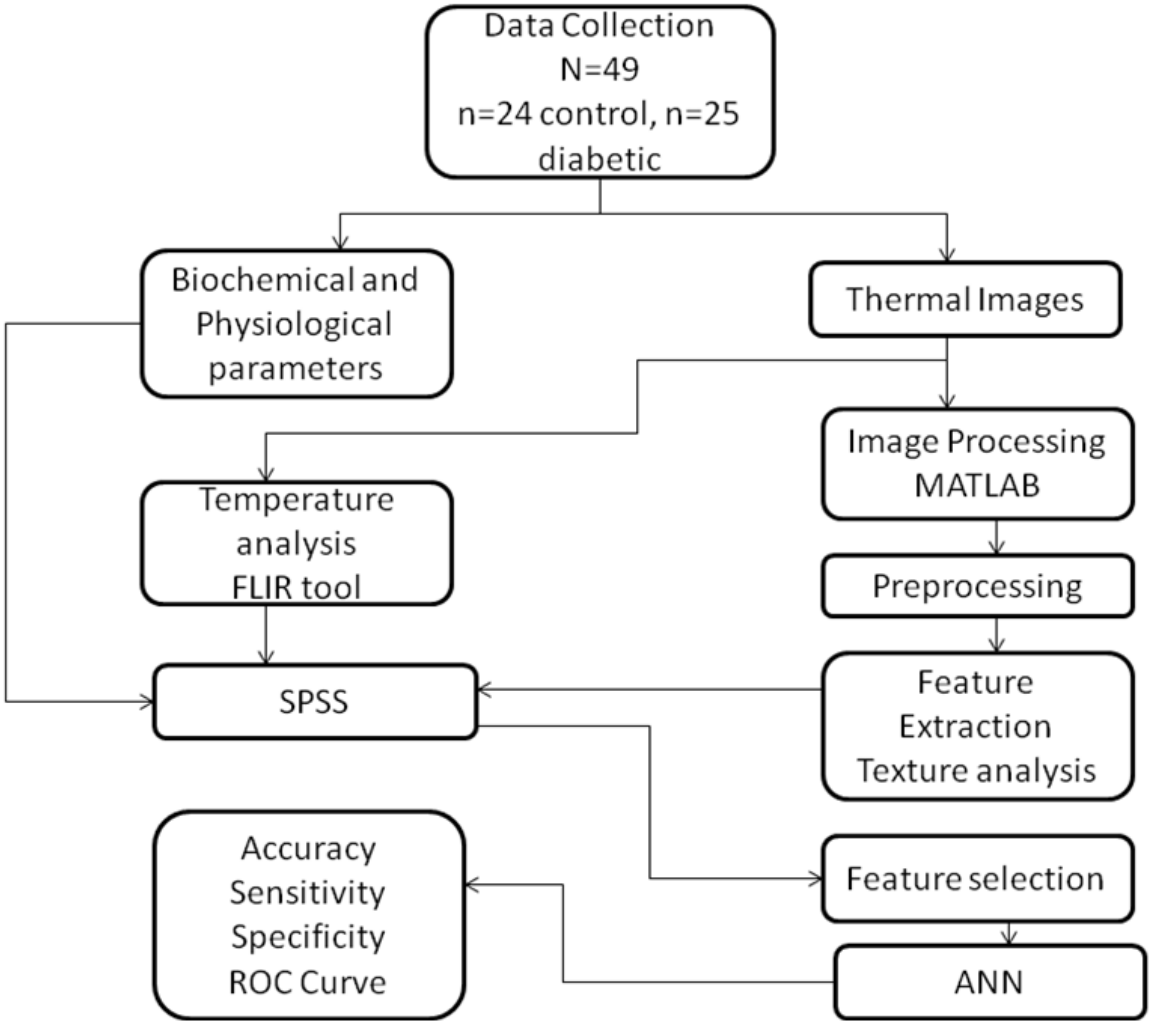

Fig.1. The flowchart describing the process of data investigation

B. Physical, Physiological and Biochemical parameters

Anthropometrical measurements height (cm), weight (Kg), neck circumference (cm), arm circumference (cm), waist circumference, and hip circumference (cm) using the standard techniques were acquired. Body mass index (BMI), Systolic blood pressure (SBP), and diastolic blood pressure (DBP) in mmHg were measured using a sphygmomanometer. The blood test results obtained the HbA_{1c} (%), TC (mg/dl), HDL (mg/dl), LDL (mg/dl), and hs-CRP (mg/dl).

C. Thermal image acquisition procedure

Thermal infrared radiation emitted by the skin surface depends on environmental conditions such as humidity, airflow, and surrounding temperature. Hence, it is an absolute necessity of thermal image acquisition that requires a controlled environment. During the thermography procedure, the study subjects are all accommodated to the controlled room temperature maintained at 23^{o}C for 15 minutes and the humidity at 40% [19]. The image acquisition room was devoid of secondary light sources like direct sunlight. The body regions of the study subjects were disrobed, and the wearing of the metallic ornaments was restricted. The thermal imaging captured at a distance of 1m from the positioning of the thermal camera (FLIR A305sc) is shown in Figure 2. The contralateral regions of the study subjects are acquired based on the region of interest (ROI).

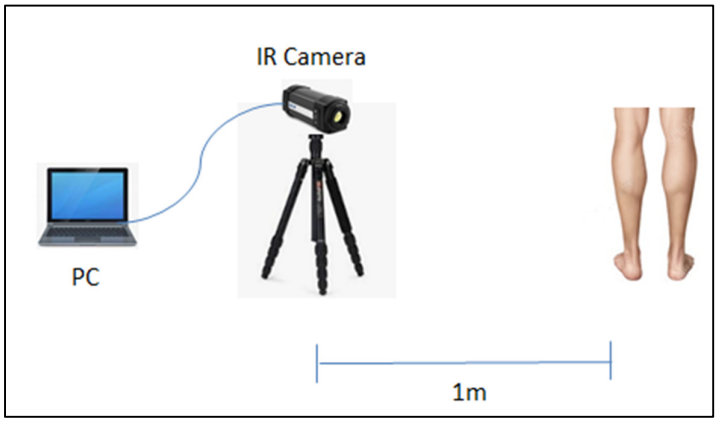

Figure 2. Thermal image acquisition system

This thermal camera operates in the spectral range of 7.5 µm – 13 µm long wavelength infrared region (LWIR); it has an IR resolution of 320×240. Further, it provides optimized image details indicating the temperature difference with thermal sensitivity of <0.05°C @ +30°C (+86°F) and Noise Equivalent Temperature Difference (NETD) of 50 mK. The camera used (FLIR A305sc) is an uncooled microbolometer, the drift due to heating is very minimal. Furthermore, the chemical coolant was used to calibrate the camera before the start of an image acquisition process.

The thermal images were captured, stored, and analyzed using FLIR thermal camera-supported software Quick Report. This software enabled various palettes (Artic, Rainbow, Grayscale, Iron, and Lava) to visualize the acquired images. Furthermore, this software has measurement tools to support the analysis of desired ROI of spot, box, ellipse, line, and delta functions to give the maximum, minimum, and average temperature of the selected ROI. The temperature scale with minimum and maximum temperature settings was used to maintain uniformity among the study images. Among the software tools for thermal images, the box tool preferred to record the mean skin surface temperature.

D. Thermal image preprocessing and analysis

The most vital part of image processing for image classification or pattern recognition is the preprocessing of the raw data of the thermal images. It is of utmost importance to eliminate the pixel artifacts and reduce noise in the image by applying a low-pass filter. The following algorithm depicts the steps to follow.

Step 1: Convert the thermal image into a grayscale image

Step 2: Crop the ROI manually

Step 4: Resize the image to 256×128 size

Step 3: Apply Averaging filter

Step 4: Adjust the contrast

Based on the analysis, the tibial region indicates statistical significance to consider the ROI of the study. Noise refers to a high spatial frequency; the averaging filter reduces the noise by applying a low-pass filter to suppress the high frequency while preserving the edges and contour [20-21]. The texture analysis was implemented over the ROI in this study to identify valuable information about the structural arrangement of the surfaces [22]. The texture analysis of an image depicts the various statistical and gray-level co-occurrence matrix (GLCM) features.

The analyzed images resulted in computerized data to study the further tests based on the Statistical Package for Social Sciences (SPSS) tool. Mean and standard deviation of all the study parameters with a statistical significance assumed at $p<0.05$. The Pearson correlation depicted among the study group indicates the correlation among the measured parameters. The independent samples t-test shows the clinical; biochemical, skin surface temperature of the body regions, and GLCM features. The receiver operating curve (ROC) analysis measured the parameter that can distinguish between two diagnostic groups. The accuracy among the biochemical parameters and surface temperature of body region for diagnosis of early vascular disorder among type 2 diabetic subjects was studied. Pearson correlation is selected to study the significant GLCM features correlated with HbA_{1c} among the diseased group.

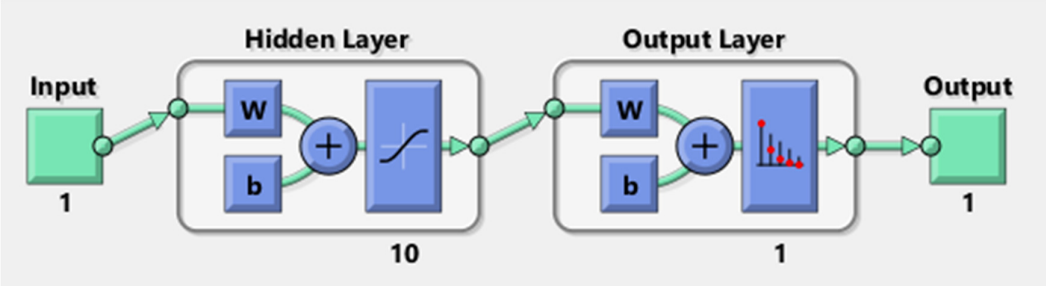

Fig.3 Architecture of the proposed Neural Network portraying the input, hidden, output layer and output neuron

The classification of subjects using a neural network from the MATLAB toolbox. The network has an input, hidden layer, output layer and output. A two-layer feed-forward network with sigmoid hidden and softmax output are used for classification. The network was trained with scaled conjugate gradient back propagation (Figure 3). The input parameters extracted from GLCM such as Entropy, Energy, Skewness, Kurtosis, Correlation and Moment 3 are used. The selected features were normalized and mapped to the bound [0, 1] and then fed to the classifier to obtain accuracy, sensitivity, and specificity.

Literature Survey

Elsayed et al., (2023) studied the standards of medical care of diabetic subjects recommended for systematic analysis of cardiovascular events. Cardiovascular diseases may have several microvascular and macrovascular complications due to uncontrolled diabetes [23]. Chu and Chen et al., (2021) developed a neural network-based CVD prediction model among the diabetic population using a Machine Learning algorithm. The results were of less acurate at 76.6% and the Area Under the Curve (AUC): 0.91. Plaque deposition under blood vessels is considered one of the serious risk factors of cardiac events, and the early detection of plaque formation may aid the therapy and prevent mortality rate. Arterial wall thermography is used as a diagnostic tool for cardiovascular diseases [24-25].

Results

As per the American Diabetes Association (ADA), the diagnostic criteria of DM was set at $HbA_{1c} \geq 6.5\%$. A total of N=49 subjects participated in the study; they were classified into control (n=24) and diabetic (n=25) based on the biochemical results. Thermal images obtained among the study group depict the temperature analysis of the contralateral regions of the various body regions such as the forehead, inner canthus, nose, neck, carotid, tympanic, palm, forearm, foot, anterior and posterior part of the knee, and tibia. The biomarkers of the following type were studied to classify and diagnose the subjects based on HbA_{1c}, lipid profile, and hs-CRP. Further, the skin surface temperature of the control subject (Figure 4) measured at the posterior view of the tibial region indicates an average skin temperature of 32.75°C.

Table 1 depicts the demography of the study parameters like age (p<0.01), SBP (p<0.05), HDL (p<0.001), HbA_{1c} (p<0.01), hs-CRP (p<0.01) and TC/HDL ratio (p<0.05) between the study groups. The analysis of the mean skin surface temperature of the tibial region of a diabetic subject indicated the temperature of 32.05°C which is 0.7°C (Figure 5) less than the diseased group with p< 0.01.

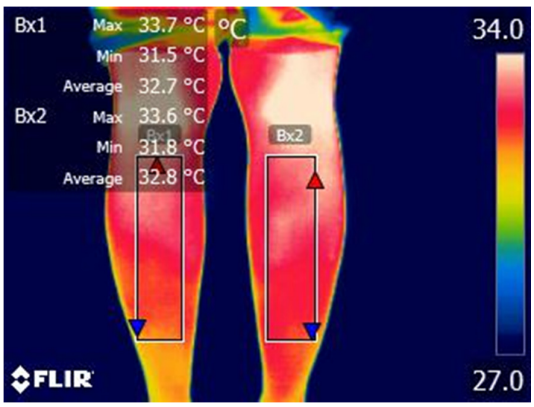

Fig.4 The tibial skin surface temperature of a healthy subject depicted the mean value of 32.75°C at the contralateral region

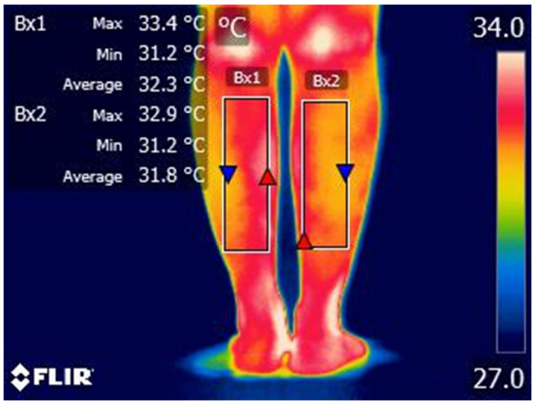

Fig.5 The tibial skin surface temperature of the CVD patient depicted a significant decrease in temperature with a mean value of 32.05ºC at the contralateral region

In this study, the hs-CRP is a low-grade inflammatory biomarker identified as a valuable tool for the risk evaluation of early cardiovascular events. Figure 6 illustrates the positive correlation between the HbA_{1c} and hs-CRP among the study group (r=0.539, p<0.01); this shows that diabetic subjects are more prone to cardiovascular events. Figure 7 demonstrates a negative correlation between inflammatory marker hs-CRP and the skin surface temperature of the tibial posterior region (r = -0.771, p<0.01) among the diseased group (Table 2). An increase in hs-CRP causes a decrease in the skin surface temperature of the posterior area of the tibia. The above-stated may be due to increased insulin resistance and stenosis of the blood vessels in the tibial artery to cause poor blood perfusion to the lower extremities.

In this study, multiple statistical parameters resulted from the ROI of the thermal images. Table 2 shows the mean and standard deviation of all the extracted features. The first moment about the mean is always zero, and six other parameters were selected based on Pearson correlation (table 3) with high significant levels with p<0.01. Entropy, highly correlated with HbA_{1c}, is a prominent parameter fed into the neural network pattern recognition tool of MATLAB software which indicated overall accuracy of 89.9%, sensitivity of 88%, and specificity of 91.7% (Figure 8).

Parameters	**Mean ± SD**		***p* value**
	Control (n=24)	***Diabetic (n=25)***	
Age (Years)	38 ± 16	55 ± 10	0.03**
[a]BMI (Kg/m^2)	26 ± 4	27 ± 5	NS
[b]WC (cm)	89 ± 10	95 ± 10	NS
[c]HC (cm)	99 ± 10	103± 11	NS
Neck (cm)	35 ± 4	34 ± 3	NS
Arm (cm)	30 ± 3	29 ± 2	NS
[d]SBP (mmHg)	115 ± 10	123 ± 20	0.05*
[e]DBP (mmHg)	75 ± 8	75 ± 16	NS
[f]TC (mg/dl)	159 ± 21	166± 52	NS
[g]HDL (mg/dl)	53 ± 14	41± 10	0.03**
[h]LDL (mg/dl)	102 ± 22	105 ± 36	NS
HbA_{1C} (%)	5.3 ± 0.3	7.9 ± 1.7	0.00**
hs- CRP (mg/dl)	0.9 ± 0.58	4.54 ± 5.64	0.00**
TC/HDL ratio	3.28 ± 1.09	4.07 ± 1.06	0.05*
Body region (ºC)			
Forehead	34.6 ± 0.64	34.4 ± 0.60	NS
Inner canthus of eye	35.5 ± 0.47	35.4 ± 0.35	NS
Nose	33.0 ± 1.24	33.1 ± 1.60	NS
Neck	34.4 ± 0.59	34.1 ± 0.57	NS
Palm	33.6 ± 1.25	33.7 ± 1.47	NS
Forearm	33.1 ± 0.70	33.3 ± 0.81	NS
Carotid	34.6 ± 0.56	34.4 ± 0.52	NS
Tympanic	35.8 ± 0.54	35.7 ± 0.44	NS
Knee Anterior	32.2 ± 0.98	32.5 ± 0.99	NS
Knee Posterior	33.2 ± 0.77	33.2 ± 0.77	NS
Tibia Anterior	32.5 ± 0.98	31.0 ± 0.79	NS
Tibia posterior	32.7± 0.79	32.1± 0.60	0.017**

Metatarsal	30.5 ± 1.82	30.5 ± 1.87	NS
Midtarsal	31.3 ± 1.60	31.2 ± 1.70	NS
Heel	30.1 ± 1.80	30.2 ± 2.12	NS

Table1. Demography of the study population

* Significance level p<0.05

** Significance level p<0.01

[a]Body mass index
[b]waist circumference
[c]Hip circumference
[d]Systolic blood pressure
[e] Diastolic blood pressure
[f]Total Cholesterol
[g]High density lipo protein
[h]Low density lipo protein

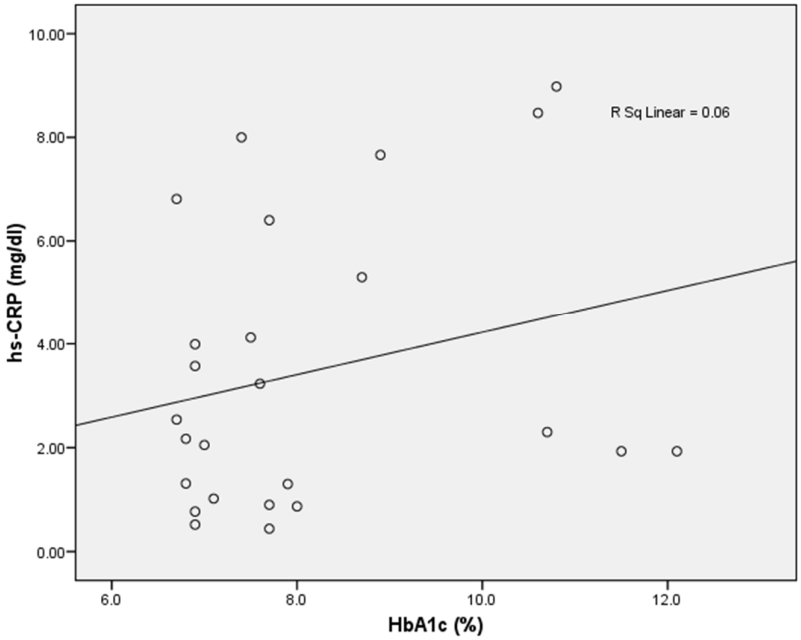

Fig.6 Pearson correlation between HbA1c (%) and hs-CRP (mg/dl)

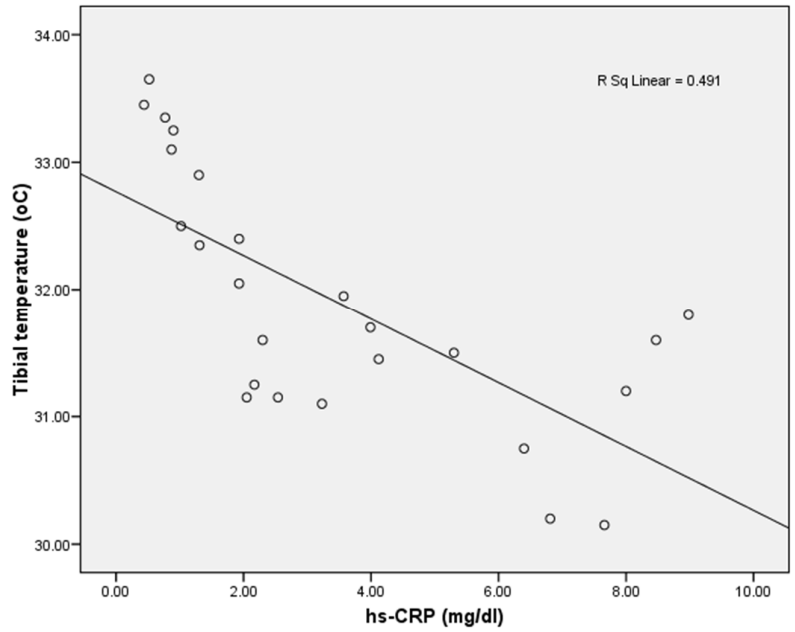

Fig. 7. Pearson correlation between hs-CRP and tibial posterior region temperature (ºC)

Table 2. Extracted features from the region of interest

Features	Mean ± SD	
	Control (n=24)	*Diabetic (n=25)*
Mean	187.59 ± 32.18	148.59 ± 32.61
STD	63.28 ± 5.39	60.41 ± 7.08
Median	204.1458 ± 43.38	152.04 ± 45.89
Energy	494049.39 ±17416	273493.60 ±101811
Skewness	-1.65 ± 0.93	-0.44 ± 0.82
Entropy	4.745 ± 0.9354	5.641 ± 0.8364
Kurtosis	5.644 ± 1.94	3.692 ± 1.27
Contrast	2.50 ± 0.977	1.51 ± 0.96
Correlation	0.47 ± 0.17	0.68 ± 0.169
ASM	0.31 ± 0.15	0.22 ± 0.11
Homogeneity	0.88 ± .031	0.85 ± 0.02
Moment 2	0.06 ± 0.014	0.05 ± 0.13
Moment 3	-0.02 ± 0.017	-0.009 ± 0.016
Moment 4	0.023 ± 0.012	0.014 ± 0.012

Table 3. Pearson correlation of the selected features versus the vital parameters

Parameters	Features selected					
	Energy	Skewness	Entropy	Kurtosis	Correlation	Moment 3
Age	-0.526**	-0.468**	-	-0.451*	0.511*	-0.555**
HbA_{1c}	-0.554**	0.504**	-0.500**	-0.515**	0.505**	0.468**
hs-CRP	-	-	-0.799**	-	-	-

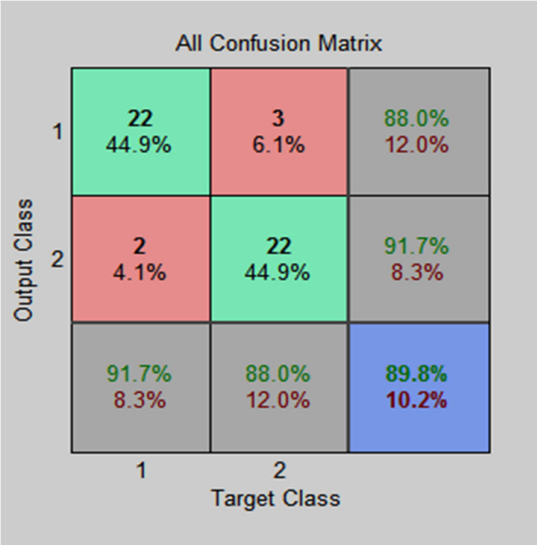

Fig. 8. The confusion matrix of the study parameters

Among the diseased group, the hs-CRP negatively correlated with the statistical feature entropy (Figure 9) to demonstrate that the diabetic subjects with high hs-CRP will have low entropy from which one can predict whether diabetic study participants are prone to any cardiovascular events. The Receiver operating characteristics curve (ROC) based on the biomarker as shown in figure 10 indicated the AUC: 0.838. The ROC curve of the non-invasive tibial anterior region (figure 11) and tibial posterior region (figure 12) represents an overall AUC of 0.694 and 0.832 of diagnostic accuracy respectively.

Discussion

It was observed from the lipid profile that there was a high prevalence of CVD among the diabetic population, in which only 36% of the diabetic population lie in the normal range of lipid profile. Srivastava et al., (2018) study revealed a similar pattern where the HDL was found to be decreased significantly among the diabetic group. The decreased in HDL pose a high risk for CVD among the diabetic subjects. Further, the cause of a diminished anti-oxidant, anti-inflammatory, and vasodilator properties also related with decreased HDL [26] [Abdissa et al., (2022)]. The positive correlation of the SBP with the HbA_{1c} indicates that the

increased blood glucose level increases the risk of atherosclerosis, which in turn leads to poor blood perfusion in the tibial region Benjamin et al., (2020), Fuchs et al., (2020) [27-29]. As hs-CRP is a low-grade inflammatory biomarker, the increase in the hs-CRP indicates inflammation due to irregular atherosclerotic plaque in the vascular intima Sharif et al., (2021) [30]. The above-stated could be due to the chronically elevated blood sugar causing a decrement in Nitric oxide (NO) production that develops plaque by obstructing the blood flow Oguntibeju (2019), Buthariu et al., (2022) [31, 32].

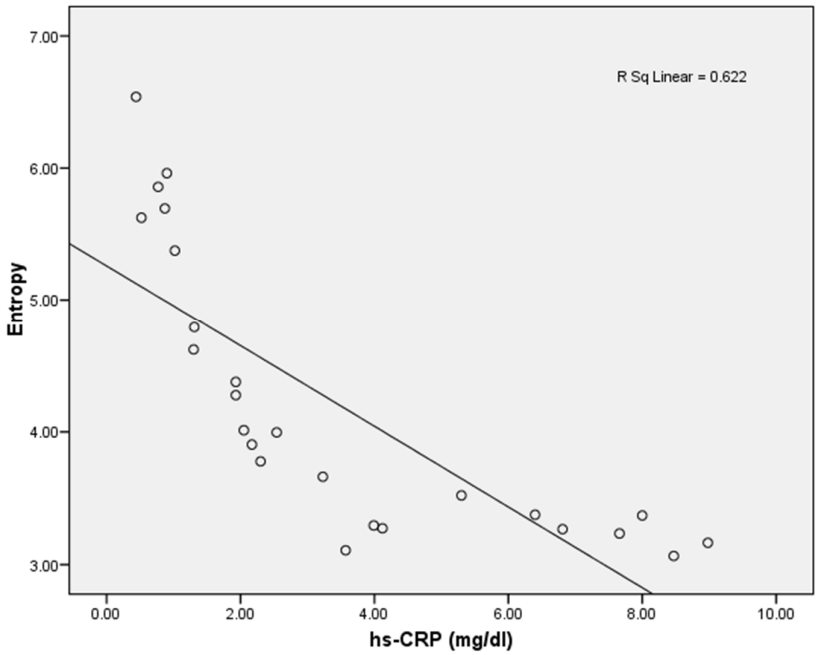

Fig. 9. Pearson correlation between hs-CRP and Entropy

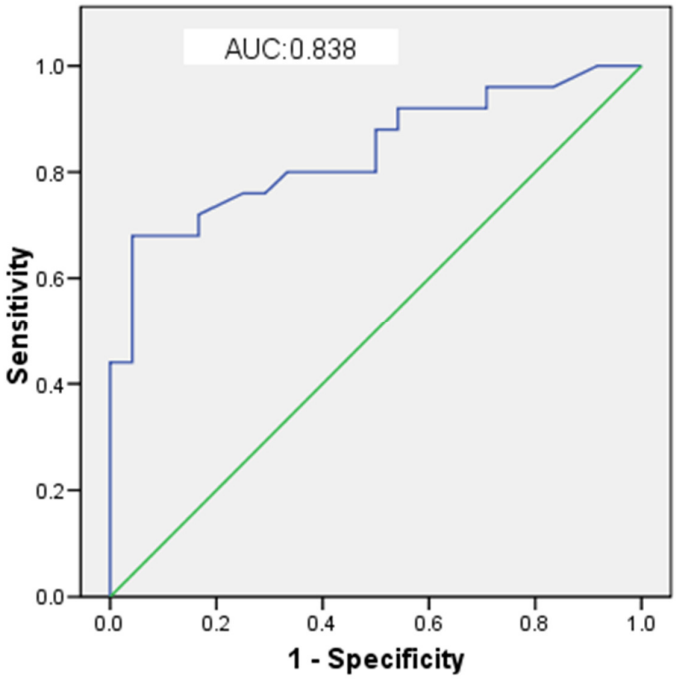

Fig 10. ROC of the hs-CRP measured from the blood sample extraction

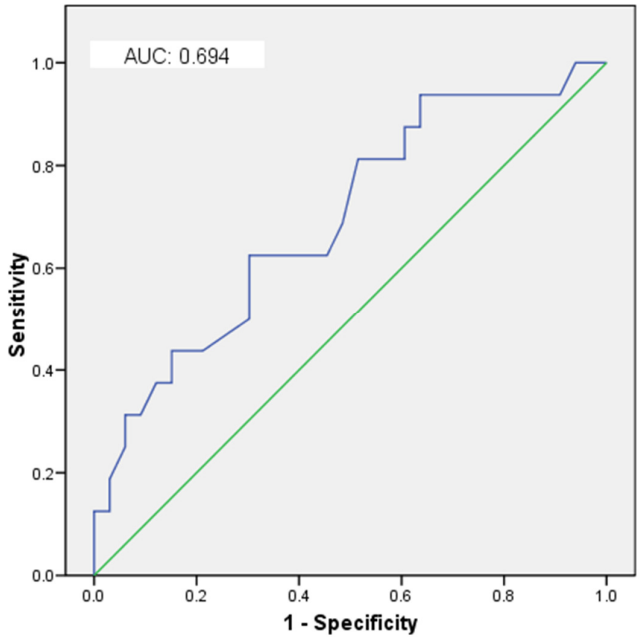

Fig11. ROC of the skin surface temperature of the Tibial (anterior) region

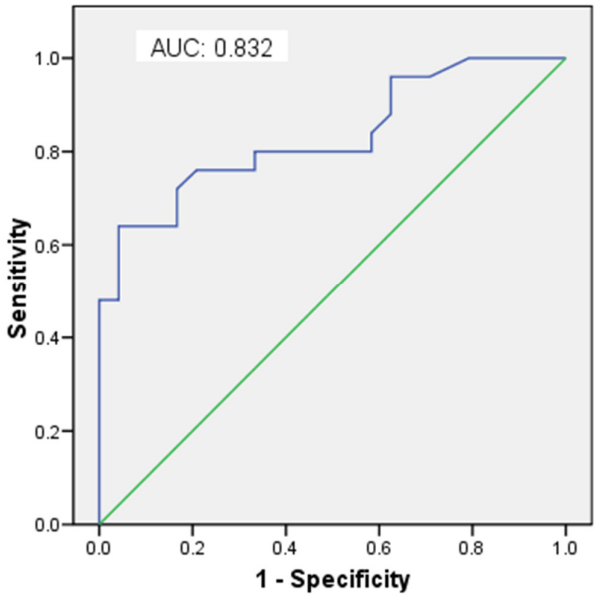

Fig12. ROC of the skin surface temperature of the Tibial (posterior) region

Although, the measured features are non-significant, the results are similar to Padierna et al (2020) study. Energy measures the textural uniformity and indicates pixel pair repetitions. It also measures the intensity of the image pixel. Hence, in the case of diabetic patients, due to the decreased temperature in the tibial region, the energy obtained was less compared to the control subject. Kurtosis measures the peak of an array of the intensity distribution. As for control subjects, the intensity distribution of Kurtosis is uniform compared to the diabetic group. Skewness measures the asymmetry of pixel distribution about its mean. The asymmetrical difference is high in diabetic subjects compared to control subjects. Furthermore, Entropy measures the randomness or uncertainty of data found to be higher among the diabetic group than in the control group [33].

Dinh et al., (2019), Khandoker (2019), and Chen et al (2017) studied non-biological parameters in diagnosis of cardiovascular disease and achieved AU-ROC score of 83.1%. These results are obtained based on the multiparameters like age, systolic blood pressure, self-reported weight, occurrence of chest pain and diastolic pressure. Whereas in the present study we used only entropy as GLCM feature extracted from skin surface temperature of the

tibial region with an accuracy of 89.8% [34]. Yan et al., (2020) worked on entropy measurement on heart rate variability with an accuracy of 81.4% that predicted the CVD risk. In the present study, entropy indicated a negative correlation with hs-CRP to predict the risk of CVD [35-37].

Conclusion

The complications of atherosclerosis cause higher morbidity and mortality in patients with diabetes mellitus. Therefore, early detection of atherosclerosis is a prime factor of concern among type 2 diabetic patients to prevent any cardiovascular events. Low-grade inflammation is linked significantly to type 2 diabetes and increases the risk of cardiovascular diseases. The hs-CRP proved to be a promising biomarker for early cardiovascular events strongly correlated with the HbA_{1c}. The average skin surface temperatures were resulted at the various regions of the study population. The skin surface temperature at the tibial posterior area depicted a significant negative correlation with hs-CRP. A decreased skin temperature of 0.6 ºC was observed at the posterior region of the tibial among the diabetic group in comparison to the control group.

The accuracy obtained from the classification in this study was 89.9%. Among the diseased group, the subjects with low entropy features haa high hs-CRP values that predict the early detection of any cardiovascular event. Thus, thermal imaging adjunct with image processing may aid as a screening tool for early diagnosis of cardiovascular events among type 2 diabetic subjects. The present work has a limitation the dataset is very limited. The machine learning approaches cannot be carried out with high accuracy. Further, control, diabetic and cardiovascular disease study subjects to be selected for future research to obtain the unbiased optimal results.

Ethical Clearance

All the procedures followed were in accordance with the ethical standards of the responsible committee on human experimentation (institutional and national) and with the Helsinki Declaration of 1975, as revised in 2000. Informed consent was obtained from all patients for being included in the study.

Conflicts of interest: The author has no conflicts of interest relevant to this article.

Funding source: This research did not receive any specific grant from funding agencies in the public, commercial, or not-for-profit sectors.

Figure Captions

Fig.1. The flowchart describing the process of data investigation

Fig.2. Thermal image acquisition system

Fig.3 Architecture of the proposed Neural Network portraying the input, hidden, output layer and output neuron

Fig 4.The tibial skin surface temperature of a healthy subject depicted the mean value of 32.75^{o}C at the contralateral region

Fig.5 The tibial skin surface temperature of the CVD patient depicted a significant decrease in temperature with a mean value of 32.05^{o}C at the contralateral region

Fig.6 Pearson correlation between HbA_{1c} (%) and hs-CRP (mg/dl)

Fig. 7. Pearson correlation between hs-CRP and tibial posterior region temperature (^{o}C)

Fig. 8. The confusion matrix of the study parameters

Fig. 9. Pearson correlation between hs-CRP and Entropy

Fig 10. ROC of the hs-CRP measured from the blood sample extraction

Fig11. ROC of the skin surface temperature of the Tibial (anterior) region

Fig12. ROC of the skin surface temperature of the Tibial (posterior) region

References

[1] Mathur P, Leburu S, Kulothungan V. (2022) Prevalence, awareness, treatment and control of diabetes in India from the countrywide National NCD Monitoring Survey. Frontiers in Public Health. Mar 14;10:205.

[2] Verhulst CE, van Heck JI, Fabricius TW, Stienstra R, Teerenstra S, McCrimmon RJ, Tack CJ, Pedersen-Bjergaard U, de Galan BE (2022). Sustained proinflammatory effects of hypoglycemia in people with type 2 diabetes and in people without diabetes. Diabetes. Dec;71(12):2716-2727.

[3] Beverly JK, and Budoff MJ. (2020) Atherosclerosis: Pathophysiology of insulin resistance, hyperglycemia, hyperlipidemia, and inflammation. Journal of diabetes. Feb 1;12(2):102-104.

[4] La Sala L, Prattichizzo F, Ceriello A. (2019) The link between diabetes and atherosclerosis. European journal of preventive cardiology. Dec 1; 26(2_suppl):15-24.

[5] Hassaan A, El-Ghany A, Mohamed I, Eldars W, Othman TA. (2022) Correlation between Highly Sensitive C Reactive Protein and Development of Microvascular Complications of Type 2 Diabetes Mellitus. Egyptian Journal of Medical Microbiology. Jan 1;31(1):69-73.

[6] Tian R, Tian M, Wang L, Qian H, Zhang S, Pang H, Liu Z, Fang L, Shen Z. (2019) C-reactive protein for predicting cardiovascular and all-cause mortality in type 2 diabetic patients: A meta-analysis. Cytokine. May 1;117:59-64.

[7] Aberra T, Peterson ED, Pagidipati NJ, Mulder H, Wojdyla DM, Philip S, Granowitz C, Navar AM. (2020). The association between triglycerides and incident cardiovascular disease: what is “optimal”?. Journal of clinical lipidology. Jul 1;14(4):438-447.

[8] Sillars A, and Sattar N (2019). Management of lipid abnormalities in patients with diabetes. Current Cardiology Reports. Nov;21:1-8.

[9] Natarajan P, Collier TS, Jin Z, Lyass A, Li Y, Ibrahim NE, Mukai R, McCarthy CP, Massaro JM, D'Agostino RB, Gaggin HK. (2019) Association of an HDL apolipoproteomic score with coronary atherosclerosis and cardiovascular death. Journal of the American College of Cardiology. May 7;73(17):2135-2145.

[10] Kanmani S, Kwon M, Shin MK, Kim MK. (2019) Association of C-reactive protein with risk of developing type 2 diabetes mellitus, and role of obesity and hypertension: a large population-based Korean cohort study. Scientific reports. Mar 14; 9(1):4573.

[11] Ammer K, and Ring F. (2019) The thermal human body: a practical guide to thermal imaging. 1st Edition, CRC Press, Jenny Standford Publishing; ISBN: 978-981-4745-82-6.

[12] Shaikh S, Akhter N, Manza R. (2019) Current trends in the application of thermal imaging in medical condition analysis. Int. J. Innov. Technol. Explor. Eng. Jun;8(8):2708-2712.

[13] Ranosz-Janicka I, Lis-Święty A, Skrzypek-Salamon A, Brzezińska-Wcisło L. (2019). Detecting and quantifying activity/inflammation in localized scleroderma with thermal imaging. Skin Research and Technology. Mar;25(2):118-123.

[14] Yadav SS, and Jadhav SM. (2022) Thermal infrared imaging based breast cancer diagnosis using machine learning techniques. Multimedia Tools and Applications. Apr 1:1-9.

[15] Simman R, Gordon DM, Klomparens K, Aviles Jr F. Use of Multimodal Long-Wave Infrared Thermography Devices in Clinical Practice. Eplasty. 2023; 23.

[16] Gurjarpadhye AA, Parekh MB, Dubnika A, Rajadas J, Inayathullah M. (2015) Infrared imaging tools for diagnostic applications in dermatology. SM journal of clinical and medical imaging. 1(1):1.

[17] Tao LC, Xu JN, Wang TT, Hua F, Li JJ (2022). Triglyceride-glucose index as a marker in cardiovascular diseases: landscape and limitations. Cardiovascular Diabetology. Dec;21(1):1-7.

[18] Zhang J. (2022) Biomarkers of endothelial activation and dysfunction in cardiovascular diseases. Reviews in cardiovascular medicine. Feb 22;23(2):73.

[19] da Rosa SE, Neves EB, Martinez EC, Marson RA, Machado de Ribeiro dos Reis VM (2023). Association of metabolic syndrome risk factors with activation of brown adipose tissue evaluated by infrared thermography. Quantitative InfraRed Thermography Journal. May 27:1-7.

[20] Ashiba HI, Mansour HM, Ahmed HM, El-Kordy MF, Dessouky MI, El-Samie FE. (2018) Enhancement of infrared images based on efficient histogram processing. Wireless Personal Communications. Mar; 99:619-636.

[21] Cañada-Soriano M, Bovaira M, García-Vitoria C, Salvador-Palmer R, de Anda RC, Moratal D, Priego-Quesada JI (2023). Application of machine learning algorithms in thermal images for an automatic classification of lumbar sympathetic blocks. Journal of Thermal Biology. Apr 1;113:103523.

[22] Almeida MA, Santos IA. (2020) Classification models for skin tumor detection using texture analysis in medical images. Journal of Imaging. Jun 19; 6(6):51.

[23] ElSayed NA, Aleppo G, Aroda VR, Bannuru RR, Brown FM, Bruemmer D, Collins BS, Das SR, Hilliard ME, Isaacs D, Johnson EL. (2023). Cardiovascular disease and risk management: standards of care in diabetes—2023 Diabetes Care. Jan 1;46(Supplement_1):S158-190.

[24] Chu H, Chen L, Yang X, Qiu X, Qiao Z, Song X, et al (2021). Roles of anxiety and depression in predicting cardiovascular disease among patients with type 2 diabetes mellitus: a machine learning approach. Front Psychol.12:1189.

[25] de Deus Passos M, Da Rocha AF (2022). Evaluation of infrared thermography with a portable camera as a diagnostic tool for peripheral arterial disease of the lower limbs compared with color Doppler ultrasonography. Archives of Medical Sciences. Atherosclerotic Diseases.;7:e66.

[26] Srivastava RA (2018). Dysfunctional HDL in diabetes mellitus and its role in the pathogenesis of cardiovascular disease. Molecular and cellular biochemistry. Mar;440(1-2):167-187.

[27] Abdissa D, Hirpa D (2022). Dyslipidemia and its associated factors among adult diabetes outpatients in West Shewa zone public hospitals, Ethiopia. BMC Cardiovascular Disorders. Feb 11;22(1):39.

[28] Hayfron-Benjamin CF, Maitland-van der Zee AH, van den Born BJ, Amoah AG, Meeks KA, Klipstein-Grobusch K, Schulze MB, Spranger J, Danquah I, Smeeth L, Beune EJ. (2020) Association between C reactive protein and microvascular and macrovascular dysfunction in sub-Saharan Africans with and without diabetes: the RODAM study. BMJ Open Diabetes Research and Care. Jul 1;8(1):e001235.

[29] Fuchs FD, Whelton PK (2020). High blood pressure and cardiovascular disease. Hypertension. Feb;75(2):285-292.

[30] Sharif S, Van der Graaf Y, Cramer MJ, Kapelle LJ, de Borst GJ, Visseren FL, Westerink J. (2021) Low-grade inflammation as a risk factor for cardiovascular events and all-cause mortality in patients with type 2 diabetes. Cardiovascular diabetology. Dec;20(1):1-8.

[31] Oguntibeju OO. (2019) Type 2 diabetes mellitus, oxidative stress and inflammation: examining the links. International journal of physiology, pathophysiology and pharmacology.11(3):45.

[32] Butnariu LI, Gorduza EV, Florea L, Țarcă E, Moisă ȘM, Tradafir LM, Cojocaru E, Luca AC, Stătescu L, Bădescu MC. (2022) The Genetic Architecture of the Etiology of Lower Extremity Peripheral Artery Disease: Current Knowledge and Future Challenges in the Era of Genomic Medicine. International Journal of Molecular Sciences. Sep 9;23(18):10481.

[33] Padierna LC, Amador-Medina LF, Murillo-Ortiz BO, Villaseñor-Mora C (2020). Classification method of peripheral arterial disease in patients with type 2 diabetes mellitus by infrared thermography and machine learning. Infrared Physics & Technology. Dec 1;111:103531.

[34] Dinh A, Miertschin S, Young A, Mohanty SD (2019). A data-driven approach to predicting diabetes and cardiovascular disease with machine learning. BMC Med Inform Decis Mak. Nov 6;19(1):211. doi: 10.1186/s12911-019-0918-5. PMID: 31694707; PMCID: PMC6836338.

[35] Yan X, Zhang L, Li J, Du D, Hou F (2020). Entropy-based measures of hypnopompic heart rate variability contribute to the automatic prediction of cardiovascular events. Entropy. 2020 Feb 20;22(2):241.

[36] Khandoker AH, Al Zaabi Y, Jelinek HF (2019). What can tone and entropy tell us about risk of cardiovascular diseases?. In2019 Computing in Cardiology (CinC) Sep 8 (pp. Page-1). IEEE.

[37] Chen C, Jin Y, Lo IL, Zhao H, Sun B, Zhao Q, Zheng J, Zhang XD (2017). Complexity Change in Cardiovascular Disease. Int J Biol Sci. Oct 17;13(10):1320-1328. doi: 10.7150/ijbs.19462. PMID: 29104498; PMCID: PMC5666530.